Title

Mini-brain computations converting dynamic olfactory inputs into orientation behavior

Author

Louis, Matthieu

Publication Date

2020-10-01

DOI

10.1016/j.conb.2019.11.015

Peer reviewed

HHS Public Access

Author manuscript

Curr Opin Neurobiol. Author manuscript; available in PMC 2021 October 01.

Published in final edited form as:

Curr Opin Neurobiol. 2020 October ; 64: 1–9. doi:10.1016/j.conb.2019.11.015.

Mini-brain computations converting dynamic olfactory inputs into orientation behavior

Matthieu Louis

Neuroscience Research Institute & Department of Molecular, Cellular, and Developmental Biology, University of California, Santa Barbara, Santa Barbara, CA 93106, USA

Department of Physics, University of California, Santa Barbara, Santa Barbara, CA 93106, USA

Abstract

The neural logic underlying the conversion of non-stationary (dynamic) olfactory inputs into odor-search behaviors has been difficult to crack due to the distributed nature of the olfactory code — food odors typically co-activate multiple olfactory sensory neurons. In the *Drosophila* larva, the activity of a single olfactory sensory neuron is sufficient to direct accurate reorientation maneuvers in odor gradients (chemotaxis). In this reduced sensory system, a descending pathway essential for larval chemotaxis has been delineated from the peripheral olfactory system down to the premotor system. Here, I review how anatomical and functional inspections of this pathway have advanced our understanding of the neural mechanisms that convert behaviorally-relevant sensory signals into orientation responses.

Transforming sensory signals into orientation behaviors

Olfaction has two main purposes: odor categorization and odor-source tracking. While the identification of an odor can be seen as an on-the-spot process that “decodes” the subset of co-activated olfactory sensory neurons, the tracking of an odor source involves the detection of temporal changes in odor concentration to organize locomotion toward the source. As movement is necessary to sample the olfactory world, sensation and behavior are intertwined in a *sensorimotor* loop [1]. The genetic tractability of the *Drosophila* nervous system [2] and its numerical tractability offers an opportunity to decipher the neural-circuit computations underlying sensorimotor integration during navigation in odor gradients (chemotaxis).

Active sampling to detect stimulus derivatives

Soon after embryonic development, *Drosophila* larvae use their sense of smell [3,4] and the computational power of ~10,000 neurons to forage on fruits in the wild [5]. Whereas many insects encounter discontinuous olfactory stimulations in plume structures while flying [6]

(mlouis@ucsb.edu).

Declaration of interest

The author declares no conflict of interest.

and walking [7], small animals like larvae tend to experience less turbulent sensory conditions due to the zero velocity of the air at the interface between the atmosphere and the substrates on which they move [8]. When exposed to smooth attractive-odor gradients, *Drosophila* larvae demonstrate precise and reproducible orientation responses (Fig. 1A) [9]. Quantification of behavior in controlled odor gradients has revealed key principles directing larval chemotaxis [9–11].

The algorithm organizing larval chemotaxis can be decomposed into elementary sensorimotor tasks [12] (Fig. 1B). In analogy with bacterial chemotaxis [13], larvae move through "runs" propelled by forward peristalsis [14] and punctuated by two types of reorientation maneuvers: (i) smooth turns ("weathervaning") in which animals gently curve toward the source during a run [15,16] and (ii) stops followed by wide-amplitude turns (stop-turns) [10,11]. Both types of turns are biased toward the local gradient as a result of lateral scans of the head (exploratory movements colored in magenta in Fig. 1A) —an active-sensing process analogous to sniffing in vertebrates [12]. Each aspect of larval chemotaxis relies on the detection of temporal changes in odor concentration (derivatives). How are these *derivatives* measured and used to orchestrate reorientation maneuvers? To address this question, *Drosophila* systems neuroscience has capitalized on the advent of complementary technologies including optogenetics [2] and computational modeling [17] to design new experimental paradigms testing mechanistic hypotheses.

Peripheral representation of dynamic stimuli in a minimalistic olfactory system

The olfactory system of the *Drosophila* larva comprises 21 olfactory sensory neurons (OSNs) that express the canonical odorant co-receptor Orco [18]. As in adult flies [19], the peripheral representation of an odor —its identity and its intensity — entails the co-activation of a subset of OSNs with different receptive fields [20,21]. Nevertheless, this "population code" is not necessary to achieve reorientation: with the information of a single OSN, larvae are capable of robust chemotaxis [9] (Fig. 1B). While some OSNs can elicit attraction on their own (e.g., the OSN expressing the odorant receptor *Or42a*) [9], others elicit repulsion (e.g., *Or49a*) [22] or no directional responses at all (unpublished observations). Thus, the core sensorimotor mechanisms guiding larval chemotaxis can be investigated in animals with an olfactory system reduced to the *Or42a* OSN alone [9]. One should nonetheless keep in mind that different OSNs are likely to direct distinct sensorimotor responses [23].

A key function of the olfactory system is to extract temporal patterns in the concentration of food-related odors. During larval chemotaxis, reorientation is triggered by stereotyped changes in odor concentration [10,11]. The detection of strong positive gradients maintain larvae in run mode. Conversely, the detection of negative gradients over several seconds promotes switches from a run to a stop-turn. During stops, head casts enable the detection of gradients on a timescale of ~500 ms [15]. Positive gradients are correlated with the "acceptance" of a head cast (conversion of a head sweep into a turn). Negative gradients are correlated with the "rejection" of a head cast by initiating a new cast [10,11]. The same logic

is thought to direct weathervaning through low-amplitude head casts executed at the end of each peristaltic cycle [15] —a active-sampling process that has recently been explored in agent-based simulations [24]. How do OSNs represent positive and negative odor gradients measured over several seconds or on shorter timescales?

Sensory features extracted by a single olfactory sensory neuron

In the “empty neuron” heterologous-expression system of the adult fly expressing the Or42a odorant receptor, prolonged odor pulses elicit transient phasic discharges followed by a lower tonic response [20]. Like other odorant receptors, the dose response of the Or42a receptor follows a sigmoidal (S-shaped) curve [20,21] expected from the biochemistry of odor binding [25]. In addition, the OSN response includes a complex phasic component revealed by carrying out electrophysiology recordings in the larval olfactory system [26]. In response to odor ramps with an amplitude and a temporal profile mirroring the sensory experience of freely-moving larvae [26] (Fig. 1C, top panel), the firing activity of the *Or42a* OSN displays nonlinear characteristics (Fig. 1C, bottom panel). While positive odor gradients evoke graded increases in firing rate, strong negative gradients repress the OSN activity below baseline (Fig. 2). Thus, a single larval OSN combines the function of an ON and an OFF detector, two operations that are usually distributed between distinct classes of sensory neurons [27]. A systematic input/output analysis has also established that the firing dynamics of the *Or42a* OSN captures the first derivative of the stimulus intensity (Fig. 2), much like the OSNs of adult flies [25,28,29].

The ability of fly OSNs to extract the temporal derivative of odorant stimuli is reminiscent of bacterial chemotaxis. *Escherichia coli* can detect temporal changes in the concentration of chemicals over five orders of magnitude [30]. Differentiation of the stimulus is underpinned by a negative feedback loop that regulates the biochemical activity of chemoreceptors [31]. This negative feedback enables bacteria to respond to the shape of the stimulus profile irrespective to its absolute intensity (fold-change-detection property) [31,32]. Whether the larval olfactory system demonstrates fold-change detection is unknown, but the activity of the larval *Or42a* OSN can be accurately described by a coarse-grained model featuring a feedforward motif [26] (Fig. 3B) capable of fold-change detection [32]. The biophysical mechanisms underlying the ability of fly OSNs to measure temporal derivatives involve adaption of the olfactory transduction cascade on a timescale of a few hundred milliseconds. In addition, the spike generation machinery of the OSN computes the derivative of the current produced by the transduction cascade [25,33]. The fact that fly OSNs display the adaptive gain-control of Weber-Fechner law [33,34] as well as adaptation to the variance of the stimulus [33,35] reminds us of the high degree of information processing that single cells are capable of [36].

Characterizing sensorimotor transformation in virtual-odor realities

Reorientation is inherently probabilistic in invertebrates [37]. In absence of olfactory stimulation, transitions from runs to stop-turns take place stochastically in the *Drosophila* larva [10,26]. To study the modulatory effects of the activity of the *Or42a* OSN on the probability of interrupting a run, it is necessary to analyze a collection of runs stimulated by the same input signal. While presenting freely-moving larvae with identical patterns of

olfactory stimulation is technically challenging with real odors [10], near-perfect control over the activity of the *Or42a* OSN can be gained in virtual realities [38] combined with optogenetics. Larvae expressing the light-gated-ion-channel channelrhodopsin [2] in their *Or42a* OSN (*Or42a*>ChR2) demonstrate strong chemotaxis (Fig. 1D) in light gradients synthesized by a closed-loop tracker [26]. Building on this paradigm, the tracker can be used to evoke the same pattern of *Or42a* OSN activity at the onset of a series of consecutive runs (Fig. 3).

Based on a linear regression between the activity of the *Or42a* OSN and the instantaneous stop-turn probability, the behavior of the larva can be predicted by a generalized linear model (GLM) [26] (Fig. 3C). Simply put, the GLM establishes that strong firing activity of the *Or42a* OSN (ON response) is a GO signal that promotes running. Conversely, inhibition of the OSN activity (OFF response) promotes stopping. Similar conclusions have been reached from reverse-correlation analyses with white-noise stimulations [39,40]. A major outcome of the GLM is that the information about the stimulus intensity and its first derivative alone are insufficient to make accurate behavioral predictions [26]. Therefore, the intracellular processing within the *Or42a* OSN achieves nonlinear-temporal computation essential for proper chemotaxis. Agent-based simulations [7,41] represent a powerful framework to test whether the combination of these mechanisms is sufficient to replicate the behavior of real animals.

Neural correlates of action selection and motor actuation

Motor programs (actions) are thought to be issued by the activation of specific descending neurons that connect the brain to the premotor system in the ventral nerve cord (VNC) of insects. Although descending neurons are frequently described as “command neurons”, it is important to appreciate that any descending neuron acts in concert with other neurons conditioning the implementation of a motor “command” [42]. The adult fly has ~550 pairs of descending neurons [43] with an anatomical organization that is well-characterized [44]. The optogenetic activation of individual descending neurons can trigger stereotyped behaviors [45]. Given that the same action can be elicited by distinct descending neurons, redundancy must exist in the function of individual descending pathways. The larva possesses a reduced set of ~50 descending neurons that has not been examined in detail yet [46].

What information does the larval brain provide?

The VNC of the larva is believed to be the site of central pattern generators underpinning peristalsis [47]. Spontaneous transitions between forward peristalsis and stops can occur in absence of the brain [48,49]. Inputs from the brain are nonetheless essential for the proper execution of stop-turns upon detection of negative odor gradients. This function is carried out in part by the PDM descending neuron (PDM-DN) downstream from the *Or42a* OSN [50] (Fig. 4Ai). Electron-microscopy (EM) of the larval nervous system [51] has enabled a systematic reconstruction of the main neuronal pathway upstream and downstream from PDM-DN [50] from its sensory afferents down to the motor system (Fig. 4Aii). Anatomical

and functional data suggest a subdivision of the PDM-DN descending circuitry into three modules.

Upstream module: sensory encoding

The main upstream partners of PDM-DN are the *Or42a* and *Or42b* OSNs —a result consistent with the fact that PDM-DN was identified in a loss-of-function screen conducted with an odor (ethyl butyrate) that preferentially activated this pair of OSNs [50]. Loss-of-function of PDM-DN does not impair chemotaxis to all odors, hinting at the existence of descending pathways downstream from OSNs that do not innervate PDM-DN. The *Or42a* and *Or42b* OSNs project onto the antennal lobe, which includes an elaborate network of interneurons [52]. Given the high-degree of information processing that takes place in the first-order *Or42a* OSN, what could be the role of the antennal lobe circuit in the sensorimotor transformation of dynamic olfactory inputs to direct chemotaxis? Electrophysiological inspections in adult flies have concluded that projection neurons (PNs) capture the derivative of the activity of their cognate OSNs [29] through a synaptic depression mechanism [53]. Since OSNs encode features related to the first derivative (speed) of the stimulus [26,28], PNs respond in part to the second derivative (acceleration) of the stimulus. Considering the architectural similarities of the antennal lobe of the larva and the adult fly [18], it is possible that the larval uniglomerular *Or42a* PN (*Or42a* uPN) encodes information related to the speed and the acceleration of the stimulus. The extraction of such features might be useful for larvae to optimize their ascent of odor gradients leading to food sources.

Central module: PDM-DN regulatory circuit

The *Or42a* uPN is connected to PDM-DN via two main routes [50]: (i) through the LH-LN1 neuron and (ii) through LH-LN2 neuron, which lies downstream from LH-LN1 (Fig. 4B). Accordingly, the LH-LN1 and LH-LN2 neurons form a feedforward motif [54]. Whether the interactions between elements of this microcircuit are excitatory or inhibitory is still unknown. While awaiting the characterization of the neurotransmitters released by the LH-LN neurons, theory allows us to speculate about circuit diagrams that could produce action selection. Most larval olfactory projection neurons are cholinergic [55]. Therefore, the effect of *Or42a* uPN onto LH-LN1 is likely to be increased. In response to positive gradients activating the *Or42a* OSN and uPN, the activity of LH-LN1 must be excited. For PDM-DN to stay inactive during upgradient runs, the effect of LH-LN1 on PDM-DN must be inhibitory. By extension, it is reasonable to assume that LH-LN1 has an inhibitory effect on LH-LN2. Under these assumptions, we are left with two possible circuit diagrams (Fig. 4C): either LH-LN2 has an excitatory or an inhibitory effect on PDM-DN, which corresponds to a coherent and an incoherent feedforward (FF) loop according to the nomenclature introduced by Alon [54]. Although the dynamical properties of these two circuit motifs remain unresolved, an inhibitory interaction from LH-LN2 onto PDM-DN does not seem compatible with PDM-DN excitation at low activity of LH-LN1 during downgradient runs (Fig. 4C). Therefore, we speculate that a coherent feedforward loop might provide a core mechanism for action selection (Fig. 4C, top panel). If one envisions the possibility that LH-LN1 has antagonistic effects on LH-LN2 and PDM-DN [56], then other motifs should be considered. In view of the computation achieved by a single sensory neuron (Fig. 3B), we

cannot rule out that action selection mostly results from physiological properties of PDM-DN itself. These questions are left to be addressed in future work.

Downstream module: motor-actuation and more

The larval body can be partitioned into the head region, three thoracic and eight abdominal segments including the tail region [14]. Forward crawling results from the propagation of peristaltic waves of muscle contraction along the posterior-to-anterior axis (think about the familiar stride pattern of a caterpillar). The optogenetic activation of PDM-DN triggers deterministic stops [50]. During prolonged excitation of PDM-DN, peristalsis remains arrested but lateral head casts are released. How can two apparently mutually exclusive actions —stops and head movements — coexist? The majority of the active presynaptic sites of PDM-DN are located in the suboesophageal zone (SEZ), a premotor area interfacing the brain lobes and the VNC (Fig. 4Ai). PDM-DN is cholinergic and it synapses onto several downstream partners in the SEZ, including the GABAergic descending neuron SEZ-DN1 (Fig. 4B). The axon terminals of SEZ-DN1 lie in the VNC region where they project onto the segmentally repeated network of A27h premotor neurons whose activity is correlated with forward peristalsis [57]. Remarkably, the inhibitory action of SEZ-DN1 onto the A27h neurons is restricted to the posterior (tail) segments of the VNC. This permits a block of the initiation of peristaltic waves while enabling contractions of the thoracic segments to produce head casting [50].

Besides the sensory mechanisms that directly gate the activation of specific descending pathways, the SEZ has emerged as a multisensory premotor hub that participates in the selection between competing actions related to locomotion and feeding [58,59]. In agreement with this model, the SEZ is compartmentalized into distinct sensory modalities [60]. While much remains to be discovered about the functional organization of the SEZ, a refined and more selective activation of multiple active descending pathways might result from a winner-take-all dynamics within the SEZ circuitry [61]. As for the control of courtship behavior in adult flies [62], it is also possible that a threshold-based mechanism within PDM-DN itself contributes to the selective activation of different motor programs.

Outlook: deciphering the making of adaptive sensory decisions

Larval chemotaxis is striking due its persistency and reproducibility across individuals. In most olfactory assays, no food is found at the peak of the odor gradient. And yet foraging larvae are drawn back to the odor source for minutes if not longer. As the effects of starvation grow stronger, larvae eventually lose interest in the “deceitful” odor and search for another potential food source [3]. Habituation to the irrelevant odor might arise from a process called “negative image” [63] implemented by local inhibitory interneurons in the antennal lobe [52]. A gradual loss of interest in the odor might also result from neuromodulation via the neuropeptide F and dopaminergic neurons [64] in a mechanism similar to the modulation of odor-search persistency in adult flies [65]. Finally, larvae are capable of associative conditioning [66] during their interactions with the environment. Individual aspects of the sensorimotor control of larval chemotaxis (e.g., the ability to turn while moving down-gradient, Fig. 1B) can be gradually tuned to produce enhanced or

reduced attraction to a given odor [67]. Where and how the innate and learned olfactory pathways interact to produce adaptive sensorimotor transformation is a fascinating problem that can now tackled by combining electron microscopy, functional imaging, behavioral inspections and computational modeling [68,69].

Acknowledgements

I am grateful to K. Nagel, J. Simpson, D. Tadres and I. Tastekin for helpful comments on the manuscript. I thank I. Tastekin for producing the images of Fig. 4A. Due to space constraints, this review is focused on “innate” larval chemotaxis. Many publications related to adult-fly olfaction, larval thermotaxis and larval phototaxis could not be cited here. These papers have nonetheless been inspirational to our understanding of larval chemotaxis. This work was funded by a University of California Regents’ Junior Faculty Fellowship Award and the NIH Brain Initiative (R01-NS113048).

References

1. Huston SJ, Jayaraman V: Studying sensorimotor integration in insects. Current opinion in neurobiology 2011, 21:527–534. [PubMed: 21705212]
2. Simpson JH, Looger LL: Functional imaging and optogenetics in Drosophila. Genetics 2018, 208:1291–1309. [PubMed: 29618589]
3. Asahina K, Pavlenkovich V, Vosshall LB: The survival advantage of olfaction in a competitive environment. Current Biology 2008, 18:1153–1155. [PubMed: 18674910]
4. Almeida-Carvalho MJ, Berh D, Braun A, Chen Y-c, Eichler K, Eschbach C, Fritsch PM, Gerber B, Hoyer N, Jiang X: The Ol1mpiad: concordance of behavioural faculties of stage 1 and stage 3 Drosophila larvae. Journal of Experimental Biology 2017, 220:2452–2475. [PubMed: 28679796]
5. Soto-Yéber L, Soto-Ortiz J, Godoy P, Godoy-Herrera R: The behavior of adult Drosophila in the wild. PloS one 2018, 13:e0209917. [PubMed: 30596767]
6. Cardé RT, Willis MA: Navigational strategies used by insects to find distant, wind-borne sources of odor. Journal of chemical ecology 2008, 34:854–866. [PubMed: 18581182]
7. Álvarez-Salvado E, Licata AM, Connor EG, McHugh MK, King BM, Stavropoulos N, Victor JD, Crimaldi JP, Nagel KI: Elementary sensory-motor transformations underlying olfactory navigation in walking fruit-flies. Elife 2018, 7:e37815. [PubMed: 30129438] [**] This paper presents a detailed quantitative analysis of the orientation algorithm directing odor-attraction behavior in walking adult flies monitored in controlled olfactory environments. Odor-evoked behaviors are decomposed into ON and OFF responses. The authors unravel the effects of the intensity and history of the odorant stimulus on these two elementary responses. Computational modeling is used test the consistency of the basic sensorimotor mechanisms that are proposed to direct odor tracking in walking flies.
8. Vogel S: Life in moving fluids: the physical biology of flow: Princeton University Press; 1996.
9. Louis M, Huber T, Benton R, Sakmar TP, Vosshall LB: Bilateral olfactory sensory input enhances chemotaxis behavior. Nature neuroscience 2008, 11:187. [PubMed: 18157126]
10. Gershow M, Berck M, Mathew D, Luo L, Kane EA, Carlson JR, Samuel AD: Controlling airborne cues to study small animal navigation. Nature methods 2012, 9:290. [PubMed: 22245808]
11. Gomez-Marin A, Stephens GJ, Louis M: Active sampling and decision making in Drosophila chemotaxis. Nat Commun 2011, 2:441. [PubMed: 21863008]
12. Gomez-Marin A, Louis M: Active sensation during orientation behavior in the Drosophila larva: more sense than luck. Curr Opin Neurobiol 2012, 22:208–215. [PubMed: 22169055]
13. Berg HC: E. coli in Motion: Springer Science & Business Media; 2008.
14. Heckscher ES, Lockery SR, Doe CQ: Characterization of Drosophila larval crawling at the level of organism, segment, and somatic body wall musculature. Journal of Neuroscience 2012, 32:12460–12471. [PubMed: 22956837]
15. Gomez-Marin A, Louis M: Multilevel control of run orientation in Drosophila larval chemotaxis. Frontiers in behavioral neuroscience 2014, 8:38. [PubMed: 24592220]

16. Iino Y, Yoshida K: Parallel use of two behavioral mechanisms for chemotaxis in Caenorhabditis elegans. Journal of Neuroscience 2009, 29:5370–5380. [PubMed: 19403805]

17. Clemens J, Murthy M: The use of computational modeling to link sensory processing with behavior in Drosophila In Decoding Neural Circuit Structure and Function. Edited by: Springer; 2017:241–260.

18. Vosshall LB, Stocker RF: Molecular architecture of smell and taste in Drosophila. Annu. Rev. Neurosci 2007, 30:505–533. [PubMed: 17506643]

19. Hallem EA, Carlson JR: Coding of odors by a receptor repertoire. Cell 2006, 125:143–160. [PubMed: 16615896]

20. Kreher SA, Mathew D, Kim J, Carlson JR: Translation of sensory input into behavioral output via an olfactory system. Neuron 2008, 59:110–124. [PubMed: 18614033]

21. Si G, Kanwal JK, Hu Y, Tabone CJ, Baron J, Berck M, Vignoud G, Samuel AD: Structured odorant response patterns across a complete olfactory receptor neuron population. Neuron 2019, 101:950–962. e957. [PubMed: 30683545] [*] Using calcium imaging, the activity of the entire repertoire of larval olfactory sensory neurons (OSNs) is characterized for a large set of odorants. The authors report that all olfactory sensory neurons share a common sigmoidal dose-response function and that their responses share similar temporal filters.

22. Ebrahim SA, Dweck HK, Stökl J, Hofferberth JE, Trona F, Weniger K, Rybak J, Seki Y, Stensmyr MC, Sachse S: Drosophila avoids parasitoids by sensing their semiochemicals via a dedicated olfactory circuit. PLoS biology 2015, 13:e1002318. [PubMed: 26674493]

23. Jung S-H, Hueston C, Bhandawat V: Odor-identity dependent motor programs underlie behavioral responses to odors. Elife 2015, 4:e11092. [PubMed: 26439011] [*] In this paper, the authors analyze the relationship between the combinatorial activation of distinct classes of olfactory sensory neurons (OSNs) and the organization of reorientation responses. The authors report that olfactory stimulations affect locomotion in a large number of ways, which depend on the nature of the odorant stimulus. In addition, different classes of OSNs modulate distinct set of motor programs, thereby suggesting that each OSN class activates a slightly different set of descending neurons.

24. Wystrach A, Lagogiannis K, Webb B: Continuous lateral oscillations as a core mechanism for taxis in Drosophila larvae. Elife 2016, 5:e15504. [PubMed: 27751233] [*] This study proposes an agent-based model that accounts for the ability of larvae to locally direct their runs toward the odor gradient (“weathervaning”, see ref. [15]). The authors make the hypothesis that active sampling through lateral head movements is underpinned by an oscillator. In spite of its simplicity, the model reproduces many essential features of larval chemotaxis, which highlights the idea that complex behavior does not necessarily arise from complex regulatory mechanisms.

25. Nagel KI, Wilson RI: Biophysical mechanisms underlying olfactory receptor neuron dynamics. Nature neuroscience 2011, 14:208. [PubMed: 21217763]

26. Schulze A, Gomez-Marin A, Rajendran VG, Lott G, Musy M, Ahammad P, Deogade A, Sharpe J, Riedl J, Jarriault D, et al.: Dynamical feature extraction at the sensory periphery guides chemotaxis. Elife 2015, 4.[**] In this comprehensive study, the response properties of a larval olfactory sensory neuron is characterized in detail by using electrophysiology combined with microfluidics to produced dynamic odor ramps. Optogenetics and closed-loop tracking are used to unravel the sensorimotor control of larval chemotaxis in virtual-odor gradients. A computational model is developed to predict the onset of reorientation maneuvers in gradients with artificial geometries. The model highlights that nonlinear information processing achieved by the olfactory sensory neurons is essential to predict behavior.

27. Tichy H, Hinterwirth A, Gingl E: Olfactory receptors on the cockroach antenna signal odour ON and odour OFF by excitation. European Journal of Neuroscience 2005, 22:3147–3160. [PubMed: 16367781]

28. Kim AJ, Lazar AA, Slutskiy YB: System identification of Drosophila olfactory sensory neurons. Journal of computational neuroscience 2011, 30:143–161. [PubMed: 20730480]

29. Kim AJ, Lazar AA, Slutskiy YB: Projection neurons in Drosophila antennal lobes signal the acceleration of odor concentrations. Elife 2015, 4:e06651.

30. Sourjik V, Wingreen NS: Responding to chemical gradients: bacterial chemotaxis. Current opinion in cell biology 2012, 24:262–268. [PubMed: 22169400]

31. Lazova MD, Ahmed T, Bellomo D, Stocker R, Shimizu TS: Response rescaling in bacterial chemotaxis. Proceedings of the National Academy of Sciences 2011, 108:13870–13875.
32. Adler M, Alon U: Fold-change detection in biological systems. Current Opinion in Systems Biology 2018, 8:81–89.
33. Gorur-Shandilya S, Demir M, Long J, Clark DA, Emonet T: Olfactory receptor neurons use gain control and complementary kinetics to encode intermittent odorant stimuli. Elife 2017, 6:e27670. [PubMed: 28653907] [**] This paper defines how adult-fly olfactory sensory neurons (OSNs) responds to naturalistic stimuli reflecting the intermittent and inpredictable nature of odor plumes. The authors find that OSNs adapt to both the mean and the variance of the stimulus. Moreover, they show that mean-dependent gain control arise from odor transduction while variance-dependent gain control is partly due to the spike-generation machinery. A biophysical model integrating these mechanisms is sufficient to account for the experimental observations.
34. Cao L-H, Jing B-Y, Yang D, Zeng X, Shen Y, Tu Y, Luo D-G: Distinct signaling of Drosophila chemoreceptors in olfactory sensory neurons. Proceedings of the National Academy of Sciences 2016, 113:E902–E911.
35. Gepner R, Wolk J, Wadekar DS, Dvali S, Gershow M: Variance adaptation in navigational decision making. eLife 2018, 7:e37945. [PubMed: 30480547] [*] Using reverse-correlation analysis, the authors investigate the computational principles enabling *Drosophila* larvae to combine signals from different sensory modalities (vision and olfaction) to control orientation responses. A notable result of this study is that the activity larval olfactory sensory neurons adapts to the variance of noisy olfactory inputs. A similar property was observed in the olfatory sensory neurons of adult flies, see ref. [33].
36. Bray D: Wetware: a computer in every living cell: Yale University Press; 2009.
37. Gordus A, Pokala N, Levy S, Flavell SW, Bargmann CI: Feedback from network states generates variability in a probabilistic olfactory circuit. Cell 2015, 161:215–227. [PubMed: 25772698]
38. Dombeck DA, Reiser MB: Real neuroscience in virtual worlds. Current opinion in neurobiology 2012, 22:3–10. [PubMed: 22138559]
39. Gepner R, Skanata MM, Bernat NM, Kaplow M, Gershow M: Computations underlying Drosophila photo-taxis, odor-taxis, and multi-sensory integration. Elife 2015, 4:e06229.
40. Hernandez-Nunez L, Belina J, Klein M, Si G, Claus L, Carlson JR, Samuel AD: Reverse-correlation analysis of navigation dynamics in Drosophila larva using optogenetics. Elife 2015, 4:e06225.
41. Davies A, Louis M, Webb B: A model of Drosophila larva chemotaxis. PLoS computational biology 2015, 11:e1004606. [PubMed: 26600460] [*] Agent-based modeling represents a valuable tool to test the consistency of working hypotheses. Using this approach, Davies *et al.* ask whether the elementary sensorimotor mechanisms reported in ref. [11] are sufficient to reproduce larval chemotaxis. Using their agent-based model, they find that larvae can still chemotax when their turns are not oriented, providing that they initiate turning while moving down-gradient. This result is reminiscent of the biased random walk directing bacterial chemotaxis. Conversely, chemotaxis in larvae is not abolished when the initiation of turning maneuvers takes place independently of the stimulus providing that the turns are oriented toward the gradient. Finally, the agent-based model provides a useful framework to investigate how learning modifies the organization of chemotaxis.
42. Yoshihara M, Yoshihara M: 'Necessary and sufficient'in biology is not necessarily necessary–confusions and erroneous conclusions resulting from misapplied logic in the field of biology, especially neuroscience. Journal of neurogenetics 2018, 32:53–64. [PubMed: 29757057] [*] The concept of "command neuron" proposed in Kupfermann and Weiss in 1978 has deeply influenced the search for the neural correlates of action selection (decision making). In this perspective article, the authors discuss the pitfalls associated with the notion that a "command neuron" must be *necessary* and *sufficient* to elicit a particular motor program. Beyond semantics, this essay touches on the logic inherent to the interpetation of loss-of-function and gain-of-function manipulations in systems neuroscience.
43. Hsu CT, Bhandawat V: Organization of descending neurons in Drosophila melanogaster. Scientific reports 2016, 6:20259. [PubMed: 26837716]
44. Namiki S, Dickinson MH, Wong AM, Korff W, Card GM: The functional organization of descending sensory-motor pathways in Drosophila. Elife 2018, 7:e34272. [PubMed: 29943730]

[*] This paper presents an exhaustive anatomical analysis of half of the entire collection of descending neurons found in adult *Drosophila*. Descending neurons are grouped into ~50 types. Each descending-neuron type is mapped from its origin in sensory neuropils of the brain to its destination in the motor neuropils of the ventral nerve cord (VCN). Anatomical facts suggest functional principles left to be tested experimentally. The VNC is organized in layers that might enable the control of mutually-exclusive behavior: walking and flying. This study complements the earlier work of ref. [43].

45. Cande J, Namiki S, Qiu J, Korff W, Card GM, Shaevitz JW, Stern DL, Berman GJ: Optogenetic dissection of descending behavioral control in Drosophila. Elife 2018, 7:e34275. [PubMed: 29943729] [*] To inspect the functions of individual descending neurons labeled by tools presented in ref. [44], the authors adopted a gain-of-function (GoF) strategy based on optogenetics in freely-moving adult *Drosophila*. Quantification of the behavioral effects that follow the activation of individual descending neurons relies on an unsupervised machine-learning methodology. While the activation of most descending neurons triggers stereotyped motor programs, significant functional redundancy is observed since the same motor program can be elicited by multiple descending neurons. Notably, this study reports that the effects of optogenetic gain-of-function manipulations is dependent on the animal's behavioral state.
46. Cardona A, Larsen C, Hartenstein V: Neuronal fiber tracts connecting the brain and ventral nerve cord of the early Drosophila larva. Journal of Comparative Neurology 2009, 515:427–440. [PubMed: 19459219]
47. Pehlevan C, Paoletti P, Mahadevan L: Integrative neuromechanics of crawling in D. melanogaster larvae. Elife 2016, 5:e11031.
48. Berni J, Pulver SR, Griffith LC, Bate M: Autonomous circuitry for substrate exploration in freely moving Drosophila larvae. Current Biology 2012, 22:1861–1870. [PubMed: 22940472]
49. Pulver SR, Bayley TG, Taylor AL, Berni J, Bate M, Hedwig B: Imaging fictive locomotor patterns in larval Drosophila. Journal of neurophysiology 2015, 114:2564–2577. [PubMed: 26311188]
50. Tastekin I, Khandelwal A, Tadres D, Fessner ND, Truman JW, Zlatic M, Cardona A, Louis M: Sensorimotor pathway controlling stopping behavior during chemotaxis in the Drosophila melanogaster larva. Elife 2018, 7:e38740. [PubMed: 30465650] [**] Using a large-scale behavioral screen, we uncover a descending neurons called PDM-DN that plays a critical role in the release of reorientation maneuvers upon detection of negative odor gradients. By combining electron microscopy and light imaging, the PDM-DN circuit is mapped from the peripheral olfactory sensory neurons down to the premotor system. Functional inspections reveal how the activity of PDM-DN produces deterministic stops without impairing exploratory movements of the head to prepare turning maneuvers.
51. Schneider-Mizell CM, Gerhard S, Longair M, Kazimiers T, Li F, Zwart MF, Champion A, Midgley FM, Fetter RD, Saalfeld S: Quantitative neuroanatomy for connectomics in Drosophila. Elife 2016, 5:e12059. [PubMed: 26990779]
52. Berck ME, Khandelwal A, Claus L, Hernandez-Nunez L, Si G, Tabone CJ, Li F, Truman JW, Fetter RD, Louis M, et al.: The wiring diagram of a glomerular olfactory system. Elife 2016, 5.
53. Nagel KI, Hong EJ, Wilson RI: Synaptic and circuit mechanisms promoting broadband transmission of olfactory stimulus dynamics. Nature neuroscience 2015, 18:56. [PubMed: 25485755]
54. Shoval O, Alon U: SnapShot: network motifs. Cell 2010, 143:326–326. e321. [PubMed: 20946989]
55. Python F, Stocker RF: Immunoreactivity against choline acetyltransferase, γ-aminobutyric acid, histamine, octopamine, and serotonin in the larval chemosensory system of Dosophila melanogaster. Journal of Comparative Neurology 2002, 453:157–167. [PubMed: 12373781]
56. Vaaga CE, Borisovska M, Westbrook GL: Dual-transmitter neurons: functional implications of co-release and co-transmission. Current Opinion in Neurobiology 2014, 29:25–32. [PubMed: 24816154]
57. Fushiki A, Zwart MF, Kohsaka H, Fetter RD, Cardona A, Nose A: A circuit mechanism for the propagation of waves of muscle contraction in Drosophila. Elife 2016, 5:e13253. [PubMed: 26880545]

58. Tastekin I, Riedl J, Schilling-Kurz V, Gomez-Marin A, Truman JW, Louis M: Role of the subesophageal zone in sensorimotor control of orientation in Drosophila larva. Current Biology 2015, 25:1448–1460. [PubMed: 25959970] [*] In this paper, we identify a small set of neurons in the subosephageal zone (SEZ) that is critical for *Drosophila* larvae to time the onset of reorientation maneuvers based on the integration of dynamic sensory inputs arising from their olfactory, visual and thermosensory systems. This work suggests that the SEZ operates as a multisensory hub —a watershed— that contributes to action selection.

59. Schoofs A, Hückesfeld S, Pankratz MJ: Serotonergic network in the subesophageal zone modulates the motor pattern for food intake in Drosophila. Journal of insect physiology 2018, 106:36–46. [PubMed: 28735009]

60. Miroschnikow A, Schlegel P, Schoofs A, Hueckesfeld S, Li F, Schneider-Mizell CM, Fetter RD, Truman JW, Cardona A, Pankratz MJ: Convergence of monosynaptic and polysynaptic sensory paths onto common motor outputs in a Drosophila feeding connectome. Elife 2018, 7:e40247. [PubMed: 30526854]

61. Hampel S, Franconville R, Simpson JH, Seeds AM: A neural command circuit for grooming movement control. Elife 2015, 4:e08758. [PubMed: 26344548]

62. McKellar CE, Lillvis JL, Bath DE, Fitzgerald JE, Cannon JG, Simpson JH, Dickson BJ: Threshold-based ordering of sequential actions during Drosophila courtship. Current Biology 2019, 29:426–434. e426. [PubMed: 30661796]

63. Ramaswami M: Network plasticity in adaptive filtering and behavioral habituation. Neuron 2014, 82:1216–1229. [PubMed: 24945768]

64. Wang Y, Pu Y, Shen P: Neuropeptide-gated perception of appetitive olfactory inputs in Drosophila larvae. Cell reports 2013, 3:820–830. [PubMed: 23453968]

65. Sayin S, De Backer J-F, Siju K, Wosniack ME, Lewis LP, Frisch L-M, Gansen B, Schlegel P, Edmondson-Stait A, Sharifi N: A Neural Circuit Arbitrates between Persistence and Withdrawal in Hungry Drosophila. Neuron 2019.

66. Gerber B, Stocker RF: The Drosophila larva as a model for studying chemosensation and chemosensory learning: a review. Chemical senses 2006, 32:65–89. [PubMed: 17071942]

67. Schleyer M, Reid SF, Pamir E, Saumweber T, Paisios E, Davies A, Gerber B, Louis M: The impact of odor–reward memory on chemotaxis in larval Drosophila. Learning & Memory 2015, 22:267–277. [PubMed: 25887280]

68. Eichler K, Li F, Litwin-Kumar A, Park Y, Andrade I, Schneider-Mizell CM, Saumweber T, Huser A, Eschbach C, Gerber B: The complete connectome of a learning and memory centre in an insect brain. Nature 2017, 548:175. [PubMed: 28796202]

69. Eschbach C, Fushiki A, Winding M, Schneider-Mizell CM, Shao M, Arruda R, Eichler K, Valdes-Aleman J, Ohyama T, Thum AS, et al.: Multilevel feedback architecture for adaptive regulation of learning in the insect brain. bioRxiv 2019:649731.

Highlights

- Anatomical map of a sensorimotor pathway guiding chemotaxis in the *Drosophila* larva
- Single olfactory sensory neurons measure behaviorally-relevant odor gradients
- Single olfactory sensory neurons combine the functions of ON and OFF detectors
- A single descending neuron can trigger the onset of reorientation maneuvers
- Circuits located in the subesophageal zone (SEZ) take part in action selection

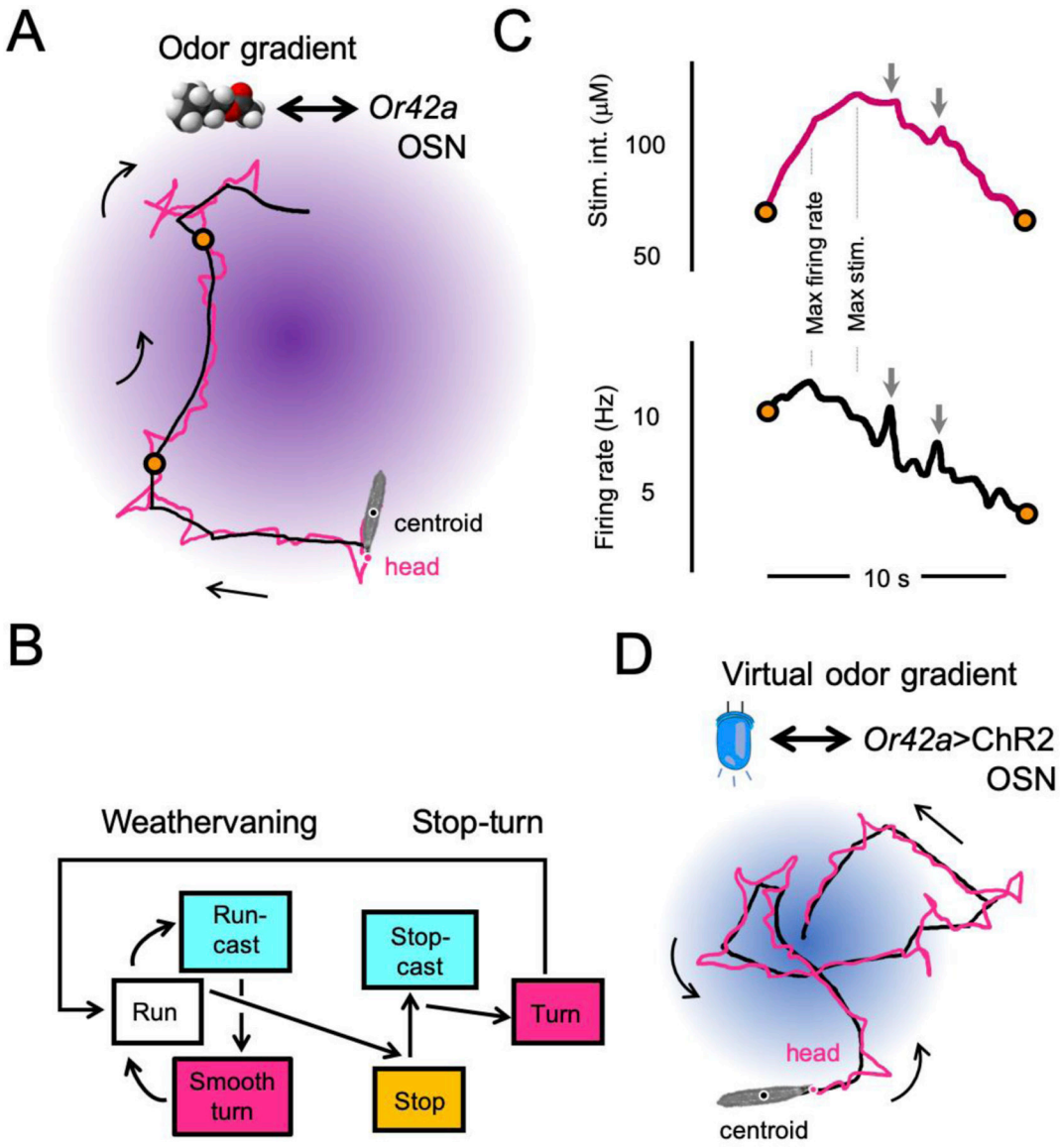

Figure 1: Larval chemotaxis in a real odor and a virtual-odor gradient.

(A) Trajectory of a larva with olfactory function restricted to the *Or42a*-expressing olfactory sensory neuron (OSN) responding to a gradient of isoamyl acetate (fruity odor). A schematic diagram of the odor gradient is depicted in purple. The positions of the centroid (black) and the head (magenta) of the larva are shown in the foreground. The two orange circles denote the turns flanking the beginning (bottom) and the end (top) of a run segment. Scale bar: the length of the larva is roughly equal to 4 mm. **(B)** Diagram of the most frequent transitions between the main behavioral programs (actions) underlying larval chemotaxis. Run-casts refer to low-amplitude lateral head movements implemented without interruption of forward peristalsis. Stop-casts refer to wide-amplitude lateral head movements occurring during stops. This diagram does not exhaustively account for all possible behavioral transitions a larva can undergo. **(C)** Time courses of the odor concentration and the *Or42a* OSN activity corresponding to the “run” segment shown in panel B. The concentration of the odor is

reported in micromolar μM (top-magenta) and the firing activity is reported in Hz (black-bottom). The time point where the stimulus intensity reaches its maximum does not correspond to the time point where the activity of the *Or42a* OSN reaches its maximum (dashed vertical lines). Localized positive gradients (gray arrows) due to lateral head casts can produce significant bursts in the firing activity of the *Or42a* OSN. **(D)** Chemotactic behavior of a larva expressing channel-rhodopsin in its *Or42a* OSN. The light gradient was produced with a closed-loop tracker. The centroid (black) and tail (magenta) positions illustrate the strong chemotactic behavior elicited by the virtual-odor gradient. Panels B-D are redrawn from [26].

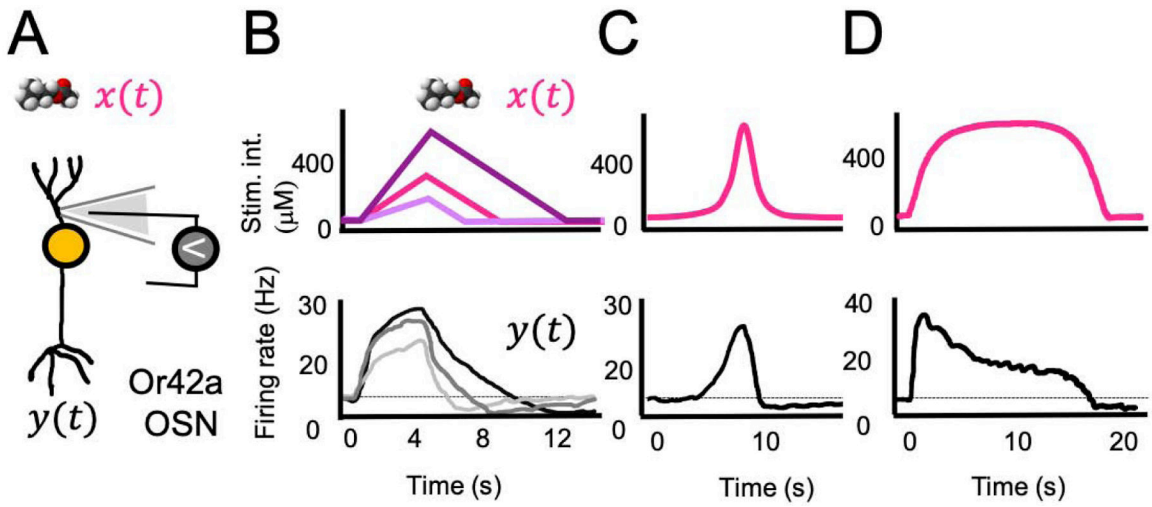

Figure 2: Response of the *Or42a* OSN stimulated by dynamic odor stimuli.

(A) Schematic diagram of *in vivo* extracellular recordings of the larval *Or42a* OSN stimulated by real odors [26]. **(B)** Stimulation of the *Or42a* OSN by symmetrical linear odor ramps with three different slopes: shallow (lilac), medium (magenta) and steep (violet). The odor ramps were produced by a microfluidics system using isoamyl acetate [26]. The duration of the upward phase is fixed to 4 s for the three ramps. The downward phase of the three ramps has the same "medium" slope, which explains differences in the time taken to complete the ramp. (Bottom) Peristimulus time histogram (PSTH) of the *Or42a*-OSN firing activity corresponding to the ramps shown in the top panel: the light to dark gray traces correspond to the shallow, the medium and the steep ramps, respectively. During the upward phase of the stimulus, the firing activity of the *Or42a* OSN reaches an asymptotic value that scales with the slope of the ramp. During the downward phase of the ramp, the OSN activity tends to follow the intensity time course, which highlights the nonlinear dimension of the *Or42a* OSN response. At the end of the ramp, the activity of *Or42a* OSN is inhibited below its basal level (dashed line). **(C)** Stimulation of the *Or42a* OSN by an exponential odor ramp. Consistent with the idea that the OSN responds to the slope of the stimulus during the upward phase of the ramp, the firing activity increases exponentially (the derivative of an exponential is an exponential). **(D)** Stimulation of the *Or42a* OSN by a "parabolic" odor ramp. During this ramp, the first derivative of the stimulus intensity decreases monotonically over time. And so does the OSN activity. Panels B-D are redrawn from [26].

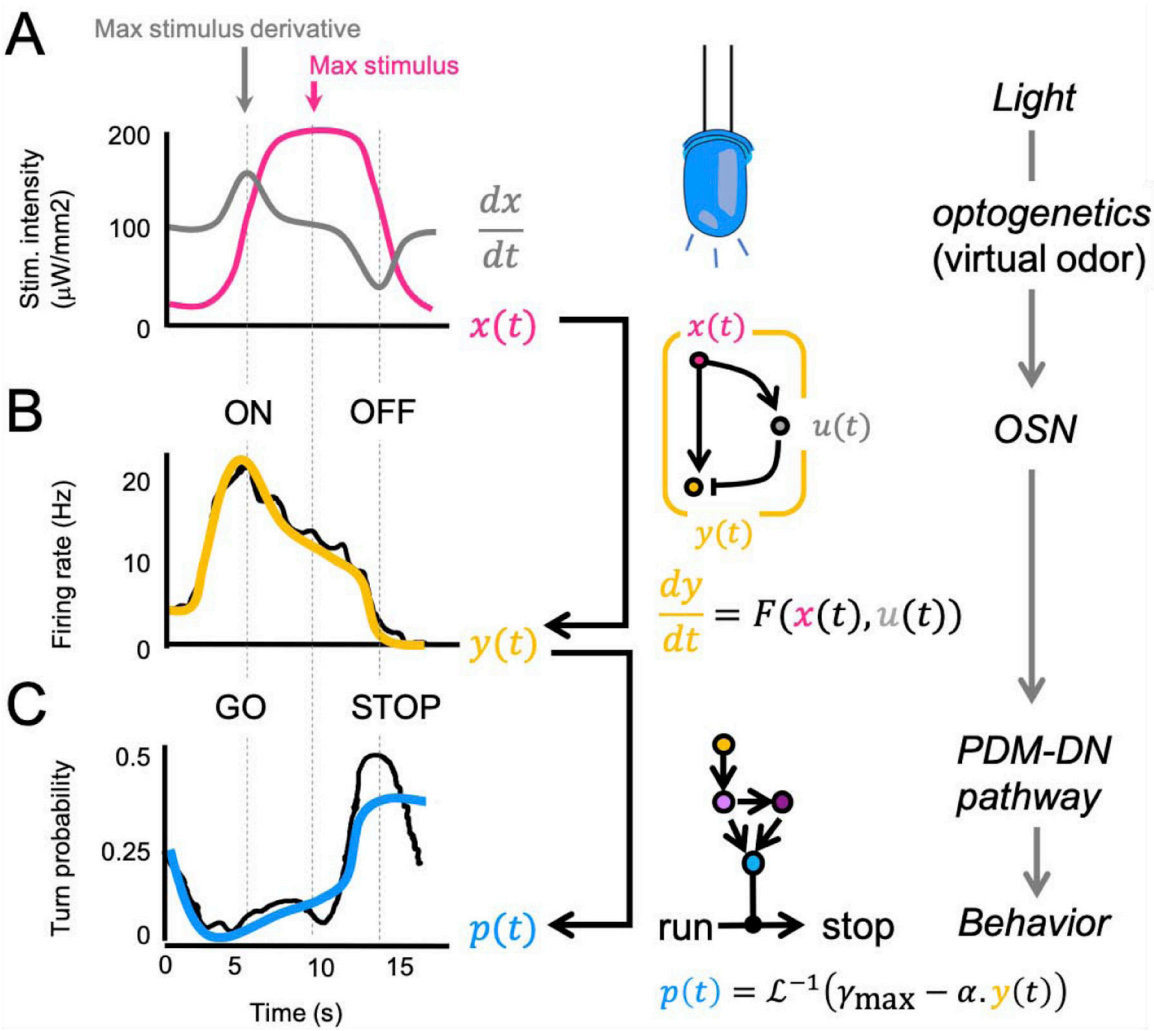

Figure 3: Computational model of the sensorimotor transformation that triggers the onset of reorientation maneuvers.

(A) Time course of a sigmoid ramp of light intensity (magenta) bearing resemblance with changes in stimulus experienced during real runs (Figure 1C). The temporal derivative of the ramp is shown in gray. **(B)** Peristimulus time histogram (PSTH) of the *Or42a* OSN expressing channel-rhodopsin (black trace) upon stimulation by the sigmoid light ramp shown in panel A. (Right) Coarse-grained biophysical model of the regulation of the firing activity of the *Or42a* OSN based on an incoherent feedforward motif (yellow diagram). The dynamics of the feedforward motif is described by an ordinary differential equation (ODE) that depends on the stimulus intensity ($x(t)$) and the activity state of an intermediate variable ($u(t)$). The molecular correlate of u remains to be determined [26]. The simulated dynamics of the ODE model is shown in yellow. **(C)** Time course of the instantaneous probability of implementing a transition from running to stopping (black trace). The probability is estimated over time bins of 1 s using a dataset of >500 runs paired with the same pattern of virtual-odor stimulation shown in panel 3A. (Bottom) Generalized linear model (GLM) of the sensorimotor transformation by the neural circuitry downstream from the *Or42a* OSN. The model predicts the probability of stopping. The linear part of the predictor combines a

positive constant ($\gamma_{\max}$) with the activity of the *Or42a* OSN ($y(t)$) multiplied by a positive constant (α). As a result, the linear predictor is equal to $\gamma_{\max}$ (max turn rate) when the activity of the OSN is suppressed during steep negative gradients whereas the linear predictor tends towards 0 (no turn) when the activity of the OSN is large during steep positive gradients. The function L^{-1} is the inverse of the *logit* linker. The predicted behavior of the GLM is shown in blue in panel C. Data shown in panels A-C are redrawn from [26].

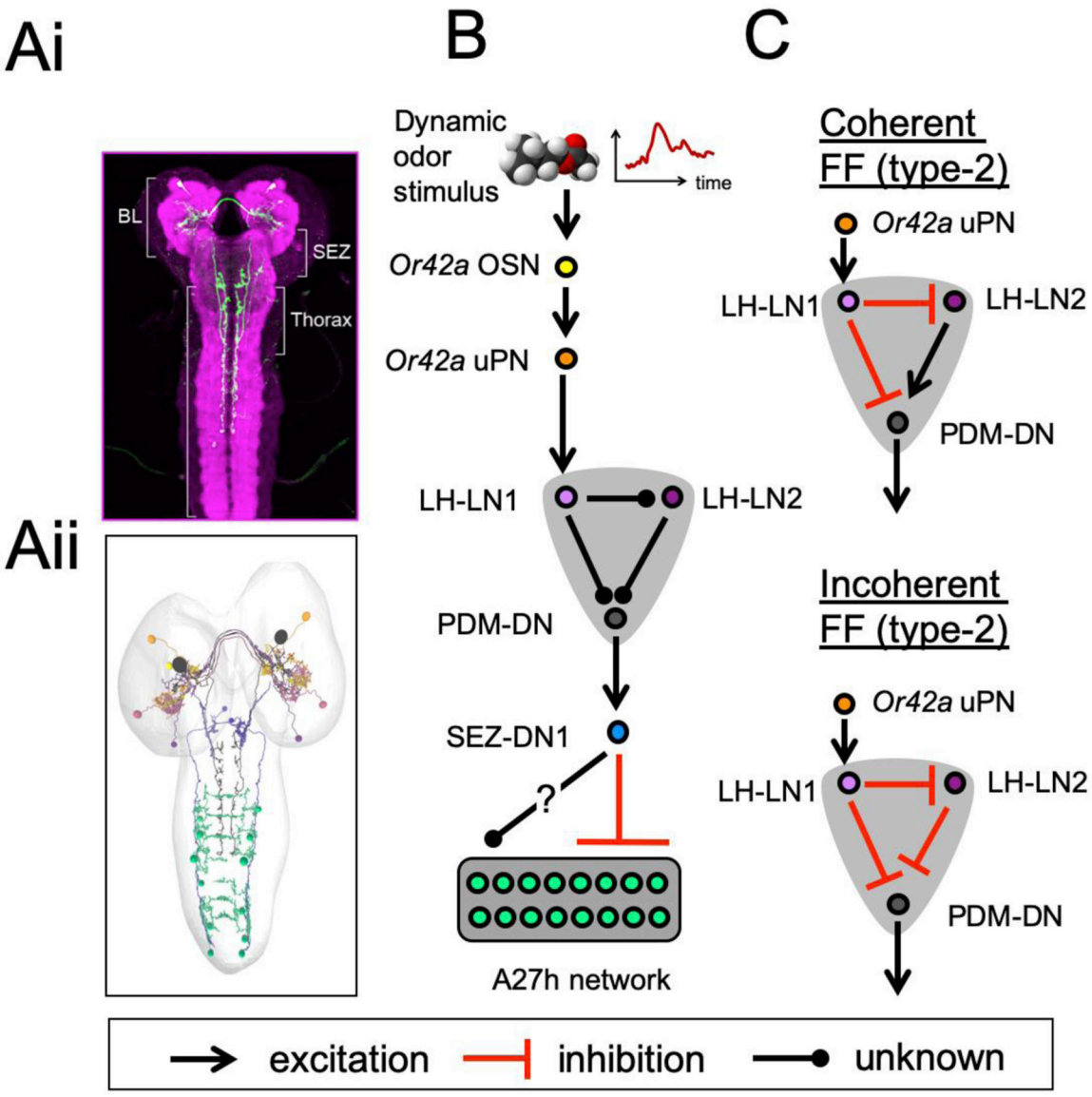

Figure 4: Sensorimotor pathway that controls run-to-stop transitions downstream from the *Or42a* OSN.

(A) Anatomy of the PDM-DN descending neuron that plays a critical role in the timing of run-to-stop transitions. The optogenetic activation of this neuron triggers near deterministic stops. In panel 4Ai, the PDM-DN neuron is labeled by the green fluorescent protein (light scanning microscopy). BL stands for brain lobes, SEZ for subesophageal zone. In panel 4ii, the main upstream and downstream partners of PDM-DN are reconstructed using electron microscopy (EM). In the EM circuit diagram, PDM-DN is labeled in black. **(B)** Outline of the main sensorimotor pathway linking PDM-DN to the pre-motor system (A27h network) and the olfactory system (*Or42a* and *Or42b* OSNs). Two neurons upstream from PDM-DN form a feedforward microcircuit. The sign (excitation/inhibition) of the edges of this diagram is still uncharacterized. PDM-DN has been shown to be cholinergic: it activates SEZ-DN1. In turn, SEZ-LN1 is GABAergic: it inhibits the activity of the A27h network thought to organize forward peristalsis. Strikingly, the inhibition is restricted to the most

posterior abdominal segments where peristalsis is initiated. The activity of SEZ-DN1 is likely to impact other motor programs through pathways that have not been traced yet (arrow with question mark). The notation convention of the interaction signs is shown at the bottom of the figure. **(C)** Hypothetical feedforward (FF) motifs of the LH-LN microcircuit directly upstream from PDM-DN. (Top) The coherent FF "type-2" (nomenclature according to [54]) assumes that LH-LN1 is inhibitory while LH-LN2 is excitatory. As a result, strong activity of *Or42a* uPN during upgradient would activate LH-LN1, which would suppress LH-LN2 and PDM-DN. Thus, negative gradients would promote the activity of PDM-DN through a release of the inhibition of LH-LN1 and/or through the disinhibition of LH-LN2. (Bottom) The incoherent FF type-2 motif assumes that both LH-LN1 and LH-LN2 are inhibitory. The expected dynamics of this motif is more ambiguous: during downgradient runs, the low activity of *Or42a* uPN is expected to release the suppression of PDM-DN by LH-LN1. At the same, low activity of LH-LN1 could enable the activity of LH-LN2, which in turn would suppress PDM-DN. This last result would be inconsistent with the fact that PDM-DN is activated during downgradient runs. Material from this figure is adapted from [50].